



Surface integrity of monocrystalline silicon nanostructured with engineered multi-tip diamond tools

Yiğit Karpata^{1,2,3} 

Received: 14 November 2021 / Accepted: 6 March 2022 / Published online: 11 March 2022
© The Author(s), under exclusive licence to Springer-Verlag London Ltd., part of Springer Nature 2022

Abstract

The ability to fabricate micro/nanostructures on large surface areas would enhance product performance in optics and solar energy systems, where maintaining high productivity is also critical. Recently, diamond tools structured with nanoscale features have been used to machine ductile materials such as copper and electroless nickel. This study uses engineered diamond tools featuring multi-tip cutting edges to investigate nanoscale grooving of silicon. Multi-tip cutting edges create a certain level of pressure and temperature at the cutting zone, which leads to phase transformations in silicon. Experiments were performed using an ultra-precision machining setup to identify conditions leading to nanoscale ductile-mode machining of silicon. As nanogrooves reach 300 nm depth, hexagonal-Si (Si-IV) phase formation was observed based on laser Raman spectroscopy measurements. Hexagonal allotropes of silicon are known to improve light absorption of silicon. Additional experiments with non-structured diamond tools did not yield any Si-IV phase transformation, indicating the importance of obtaining necessary pressure and temperature conditions at the cutting zone.

Keywords Micro/nano cutting · Diamond tool · Silicon · Phase transformation

1 Introduction

The fabrication of periodic micro and nanostructures on the surface of silicon may improve performance of various products in micro-electronics and micro-nano fluidics [1]. While non-contact processing techniques such as photolithography (electron beam, X-ray, etc.), focused ion beam (FIB) milling, and femtosecond laser machining can produce micro/nanostructures with good quality, the challenge is to fabricate those features on large surface areas with high productivity. Diamond tools with engineered cutting edges have been shown to machine nanoscale structures with high material removal rates on ductile materials such as copper and electroless nickel [2, 3]. The ability to create nanoscale features on optical materials such as silicon and germanium would

increase their optical performance which in turn increases the efficiency of the silicon-based systems.

When IR materials are machined, it is crucial to set machining parameters to maintain a phase transformation process where the semi-conductor material starts behaving like metal and produces crack-free surfaces [4]. To be able to machine silicon to have nanoscale features on the surface, it is essential to design and fabricate adequate nano features on the diamond tool and choose suitable machining conditions to machine silicon in ductile mode with these tools. Focus ion beam (FIB) milling process is commonly used to obtain nanoscale cutting edges on the single crystal diamond tools. Adjusting FIB milling parameters such as beam current, voltage, and scanning strategy is essential for obtaining desired shapes on the diamond tool tip [5]. An advantage of using FIB is that multiple nano cutting edges can be obtained at the tip of the cutting tool, thereby increasing the productivity of nanoscale machining.

Molecular dynamics (MD) simulations have been used to study deformation mechanisms of silicon. The simulation results have pointed out the importance of temperature to the dislocation movements and the resulting surface integrity [6]. Dai et al. [7] investigated the nanoscale machining of silicon with multi-tip nanostructured diamond tools using MD

✉ Yiğit Karpata
ykarpat@bilkent.edu.tr

¹ Department of Industrial Engineering, Bilkent University, Ankara, Turkey

² Department of Mechanical Engineering, Bilkent University, Ankara, Turkey

³ UNAM, Institute of Materials Science and Nanotechnology, Ankara, Turkey

simulations and found that temperature rise on the silicon during machining would be lower when structured tools are employed. Nanoscale cutting edges were also shown to cause increased friction between the tool and the silicon work material. Depending on pressure and temperature conditions that occur during deformation, silicon transforms into different phases. Paul et al. [8] calculated that range of pressure and temperature conditions for the formation of hexagonal silicon phase. According to their calculations, Si-IV phase may be formed starting from 350 K temperature and 45 GPa pressure. The viable pressure range widens to 25–70 GPa at temperature of 1000 K. Fan et al. [9] summarized possible processing routes to obtain different metastable allotropes of silicon where mechanical processing (shearing and friction) of silicon was one of them. The importance of Si-IV phase on the performance of silicon devices was reported in [10].

In this study, nanostructured diamond tools were designed and fabricated with FIB, and nanoscale machining of silicon was performed using a multi-tip, nanoscale diamond tool. The study investigates the feasibility of nanoscale machining and evaluates the influence of the nanostructured diamond tool on the surface integrity of the machined silicon. The influence of machining by non-structured diamond tools on machined surface integrity is also investigated.

2 Experimental

2.1 Fabrication of engineered multi-tip diamond tools

Diamond micro grooving tools (ALMT UPC Nano) having a width of 100 μm , 0° rake angle, and 10° clearance angle were used to obtain multi-tip, nanostructured tools. The surface of the diamond cutting tool was coated with Pt before it was processed in a FIB (FEI Quanta) device. The FIB system used a voltage of 5 kV and a probe current of 1.6 nA. In the first step of the fabrication process, the width of the tool tip is decreased via FIB from 100 to 10 μm to create (CD) the portion of the tool that will be nanostructured as shown in Fig. 1a. The design parameters of the nanostructured tools are given as: the number of teeth ($N=9$); the height of the tool tip from the base ($d=3.5 \mu\text{m}$); the width of the teeth ($b=300 \text{ nm}$); the distance between teeth ($e=600 \text{ nm}$); and the height of the teeth ($c=400 \text{ nm}$), as also shown in Fig. 1a. The width of the tool is selected relative to its height, with a ratio of 0.75. The distance between teeth is two times the width of the teeth. As a result of the interaction between FIB and diamond, some geometrical differences between designed and actual FIB-machined nanostructures, such as rounding of the edges on the corners, are likely to occur as shown in Fig. 1a. The angle Ψ , which ranges from 5–10 degrees, is due to the decreased width of

the tool (b') compared to its width at root (b). Figure 1b, c, and d shows the FIB nanostructured tool and the measurements performed with SEM under different magnifications. While it is not possible to make accurate measurements of such nano features, the height of the cutting edge was measured as 387 nm, which are slightly smaller than the design parameters of 400 nm. The width of the nano edges was measured as 300 nm as designed. In addition, non-structured diamond grooving tools with 500 μm width were also used in the experiments.

2.2 Machining setup

Machining experiments were conducted in a Moore Nanotech FG350 CNC ultra-precision diamond turning machine. A silicon workpiece with (001) crystal plane was used as the work material. A mini force dynamometer (Kistler 9256C1 and its charge amplifier connected to a data acquisition system NI 7854R A/D converter) was used to measure forces during machining tests and to detect the surface of the silicon during initial setup. In the machining experiments, the feed was set at 70 nm/rev. The cutting speed varied between 25 and 75 m/min. Figure 2 shows the experimental setup where the silicon was placed on an air chuck.

2.3 Characterization of the machined silicon surfaces

The topology of the surfaces machined with non-structured grooving tools was investigated using a laser microscope Keyence VKX 100. Those machined with nanostructured tools were inspected with micro-Raman laser spectroscopy (WITec alpha series, laser wavelength of 532 nm, and $\times 50$ objective lens with NA 0.75 resulting in $\sim 865 \text{ nm}$ laser spot size). The dimensions of the nanogrooves were measured on the same equipment using its AFM mode.

2.4 Investigation of single crystal silicon material properties using nano-indentation tests

Nano-indentation tests are suitable to identify the material properties and observe phase transformations of materials such as silicon. In this study, a Berkovich (pyramidal) type of indenter was used (Anton Paar) under various loading ranges of 5 to 50 mN and 10 to 100 mN/min loading rates. Silicon samples (001) are used in the nano-indentation tests. Mechanical properties of the material, such as modulus of elasticity (E) and Vickers hardness (HV), can be calculated based on the load vs displacement curves using Oliver and Pharr method. Based on the nano indentation test results, the modulus of elasticity (E) was measured to be around 180–200 GPa, and the hardness of the specimen was measured around 12–13 GPa.

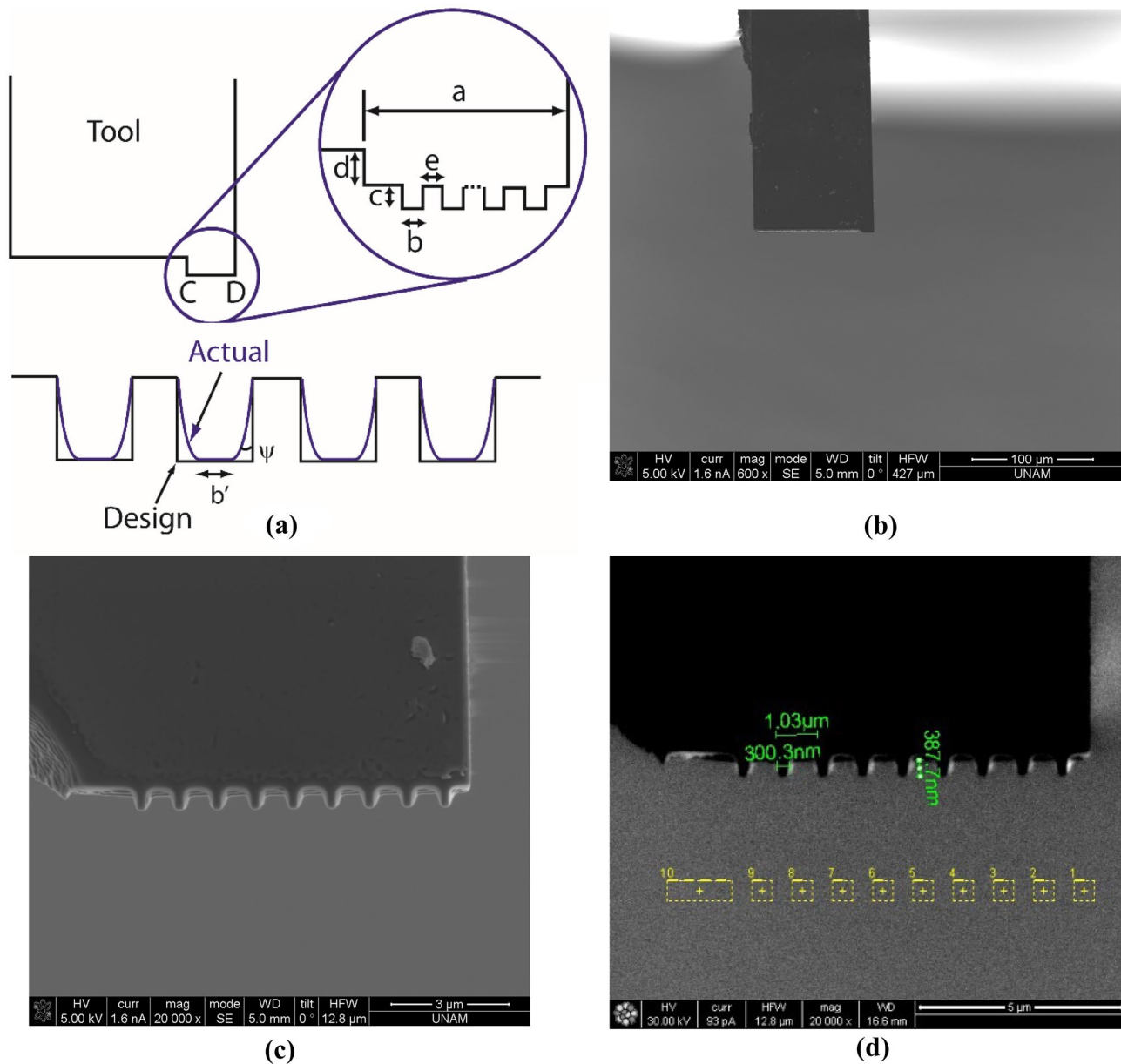


Fig. 1 (a) Design parameters of the multi-tip diamond tool, (b, c, d) nanostructured diamond tool with multi-tips under different magnifications

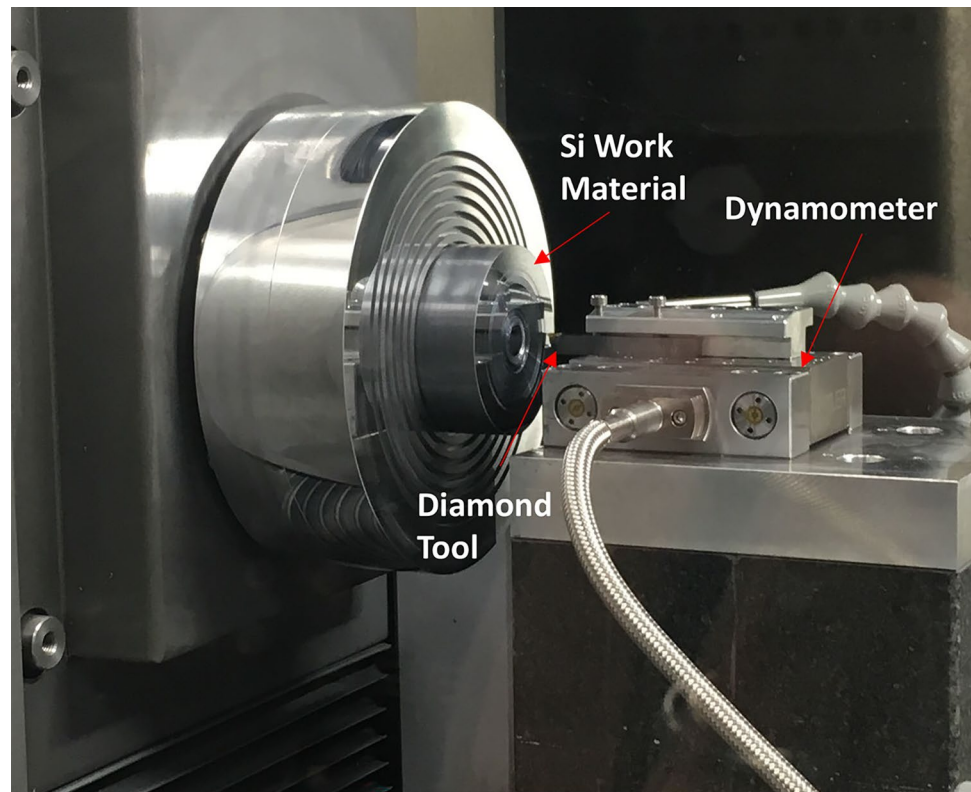
3 Results and discussion

Figure 3 shows the nanogrooves machined on the monocrystalline silicon. The nanogrooves were machined around the circumference of the work material with a length of around 78 mm. The first set of grooves represents the initial contact with the cutting edges and the work material. The marks on the surface represent ploughing conditions, where the cutting edge did not perform any machining, yet it plastically deformed the surface. The

second set of grooves represents ductile machining conditions. With increasing depth of cut on the third and fourth grooves, spalling damage on the top surface at some locations becomes visible.

Figure 4a, b show the nanochannels of the second set of grooves machined in ductile mode. The width of the groove measurements was performed with SEM, where they were measured around 200–250 nm. The measurements are quite consistent among nanochannels. The width of the nano machined grooves was smaller than the width

Fig. 2 Experimental setup on the ultra-precision turning machine



of the cutting edges which can be related to the pyramidal shape of the nano edges due to FIB processing. With material pile-up on the sides of some of the grooves, as shown in Fig. 4b, the width of the channels reached 300–350 nm. Due to the relatively large distance between the nano edges, no overlapping effect was observed.

The third and fourth sets of grooves present larger widths and depths with similar characteristics, as shown in Fig. 4c, d. With increasing depth of cut on the third and fourth set of grooves, damage on the top surface becomes visible, yet the bottoms of each channel seem to be intact. In some regions, the material on the top surface seems to be delaminated from the surface. A possible material accumulation between the surface and the root of the tool may have caused such surface defects.

Nanoscale features as large as 90 nm in height and 200 nm wide can be machined in ductile mode without material pile up. With increasing depth, grooves were obtained as deep as 300 nm. It must be noted that the flatness tolerance of the silicon work material surface, the possible tilt of the diamond tool with respect to the work material surface, and measurement uncertainties related to the nanostructured tool dimensions make it challenging to position the nanostructured tool tip on the work surface. This difficulty may impede its adoption under practical conditions.

Figure 5a shows the profiles of the nanogrooves obtained at an oblique angle after processing silicon with FIB. Figure 5b shows the AFM measurement of the surface, which shows that the depth of the grooves is around 300 nm. Based on these results, the tool design parameters and the machining conditions given here, taken together, allow transferring the shape of the tool to the silicon.

Figure 6a, b shows two different sets of nanogrooves obtained after machining. The first group, shown in Fig. 6a, had the nano cutting edges partially plunged during machining, and it presents a material pile-up region next to the grooves. As the cutting tool is further plunged, deeper nanogrooves were observed with a partially damaged layer on the top surface as shown in Fig. 6b. This damage signifies that the plastic deformation on the top surface is probably due to contact between the nano cutting edges and the cut material. Figure 6c compares the Raman spectra surfaces for different groups shown in Fig. 3. The measurements were taken from seven different locations. It must be noted that the laser spot diameter is larger than a single groove, so the measurement gives an average of both unmachined and nanoscale machined surfaces for both cases. The nanoscale grooves machined in ductile mode present a peak around 520 cm^{-1} , which corresponds to Si-I and peak around 470 cm^{-1} corresponds to amorphous a-Si. The fourth set of deeper nanogrooves presents a large peak around 300 cm^{-1} which also

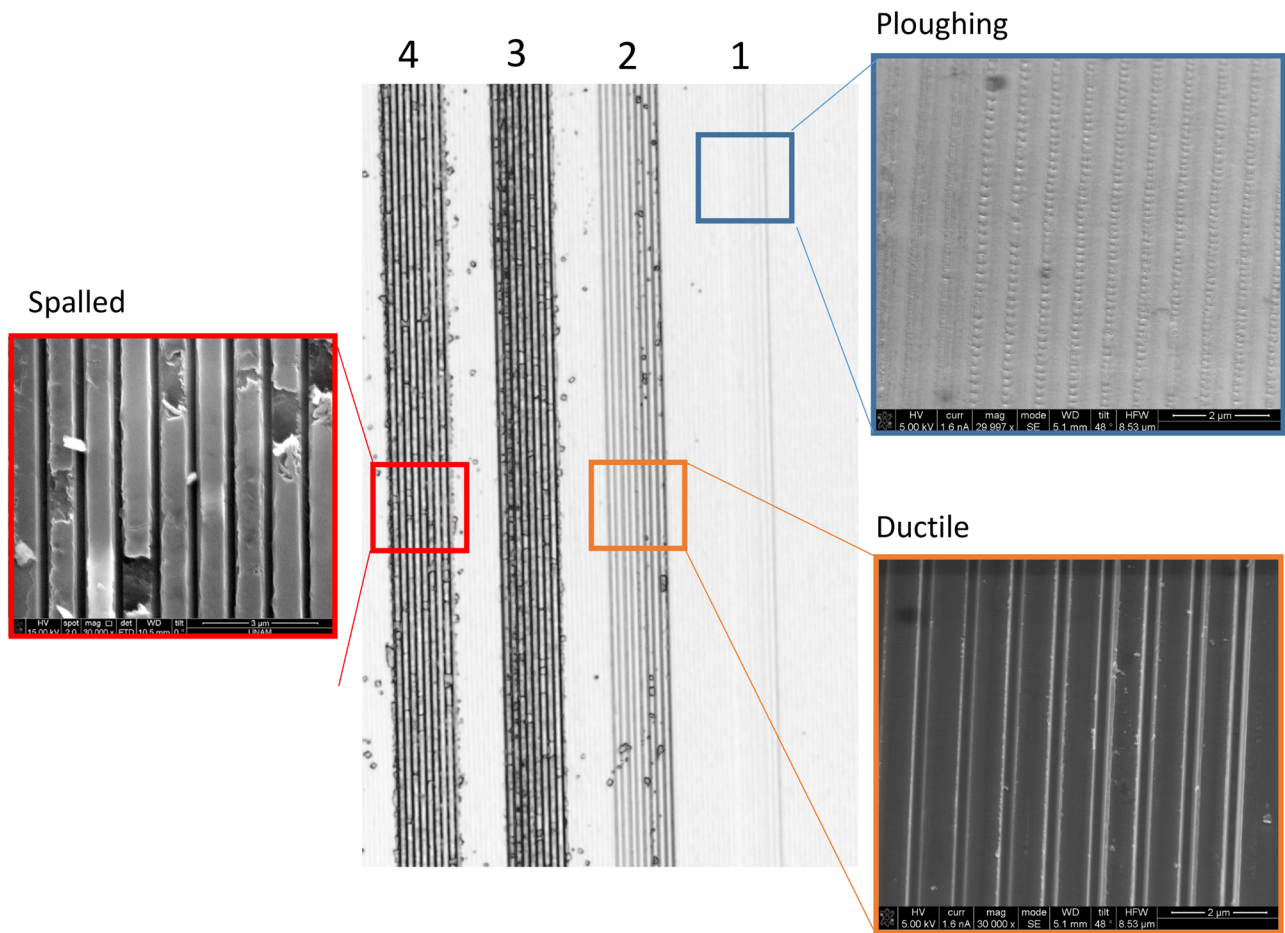


Fig. 3 Nanoscale grooves machined on the silicon surface

corresponds to a-Si. The additional (or double) peak around 496 cm^{-1} next to 520 cm^{-1} (Si-I) has been identified as Si-IV (hexagonal diamond—martensitic transformation from Si-I) in the literature [4, 11], yet another Raman band related to Si-IV at 514 cm^{-1} is not visible in the measurements. In [12], the hexagonal silicon phase has also been related to twin intersections during high-speed diamond wire scribing of silicon, creating high strain rate deformation conditions. The formation in metastable hexagonal diamond Si at twin intersections has been observed under hot indentation performed at $400\text{ }^{\circ}\text{C}$ [13]. The necessary temperature condition for hexagonal silicon formation was reported as minimum $500\text{ }^{\circ}\text{C}$ in [14] which is driven by shear stress relief. In MD simulations of nanoscale machining of silicon with nanostructured tools, it was shown that temperature rise would be around $600\text{--}650\text{ K}$ lower compared to non-structured tools [7]. The coefficient of friction would be around 1.1 which is higher than non-structured tools [7]. According to the Raman measurement intensity levels, increasing groove

depth significantly altered the surface as a deeper a-Si layer formed on the machined surface. The fractured segments of the surface may be related to the a-Si delaminating from the surface due to residual stresses.

It is difficult to measure cutting forces which would allow calculating pressured at the cutting zone during nanoscale machining with the available equipment today. To investigate the influence of micro scale non-structured tools on the surface integrity, additional machining tests were conducted where the cutting speed increased from 25 to 75 m/min to promote higher strain rate and temperature rise at the cutting zone, while keeping the feed was varied 70 to 400 nm/rev. The width of the cutting was set at $500\text{ }\mu\text{m}$ for reliable measurement forces. The groove depth was set to $20\text{ }\mu\text{m}$ during experiments. Figure 7 shows the topology of the grooves obtained after the test. Figure 7a shows the groove surface finish, which has a rms areal surface roughness (S_q) of 6 nm at 25 m/min. With increasing feed, micro cracks start to appear on the surface and rms surface roughness increases to 36 nm at 400 nm/rev.

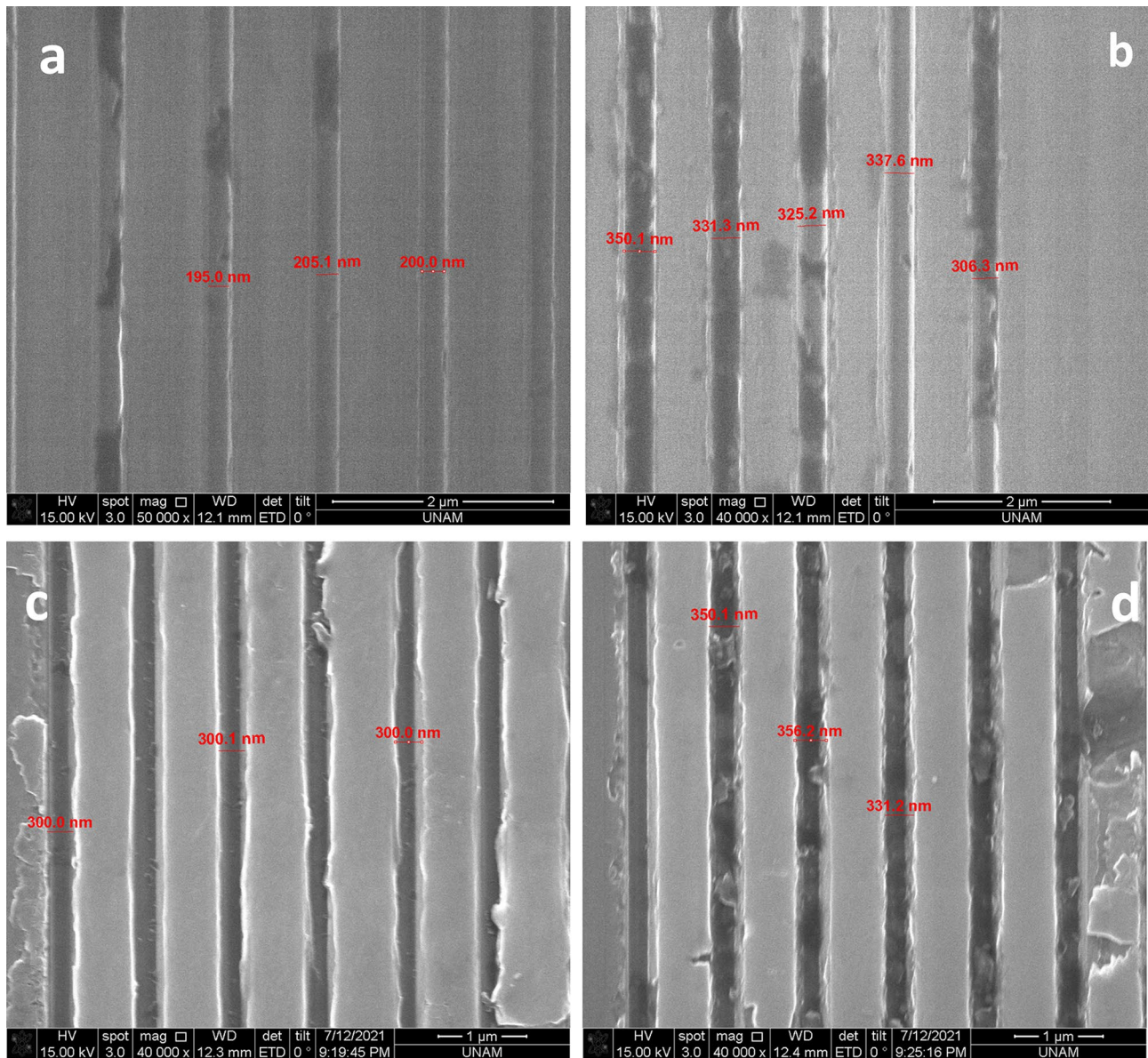


Fig. 4 Groove width measurements at different locations; (a) at the first set of grooves with ductile mode machining; (b) at the first set of grooves with material pile-up; (c) third set of grooves with material fracture; (d) fourth set of grooves with material fracture

Figure 8 shows the Raman spectra of the machined surface. Increasing the cutting speed to 75 m/min resulted in a higher peak intensity, indicating a thicker a-Si layer. A sharp peak at 520 cm^{-1} (and a minor one at 300 cm^{-1}) and no other significant peaks indicate that the structural changes are relatively small. Under the wide range of cutting conditions tested with non-structured tools, no phase transformation to Si-IV was observed. Due to fast unloading during machining tests, no transformation from Si-II to Si-III or Si-XII was observed. No phase transformation

to hexagonal silicon exists around the primary peak of 520 cm^{-1} .

Figure 9a shows the cutting and thrust force measurements during machining at 25 m/min cutting speed for different feed values. While the forces increase up to 250 nm/rev feed, the thrust force start to decline due to initiation brittle fracture. Cutting forces can be used to calculate specific cutting energy ($SCE = (F_c V)/(V \cdot w \cdot t_u)$) where F_c is the cutting force acting in the direction of cutting speed, V is the cutting speed, w is the width of cut,

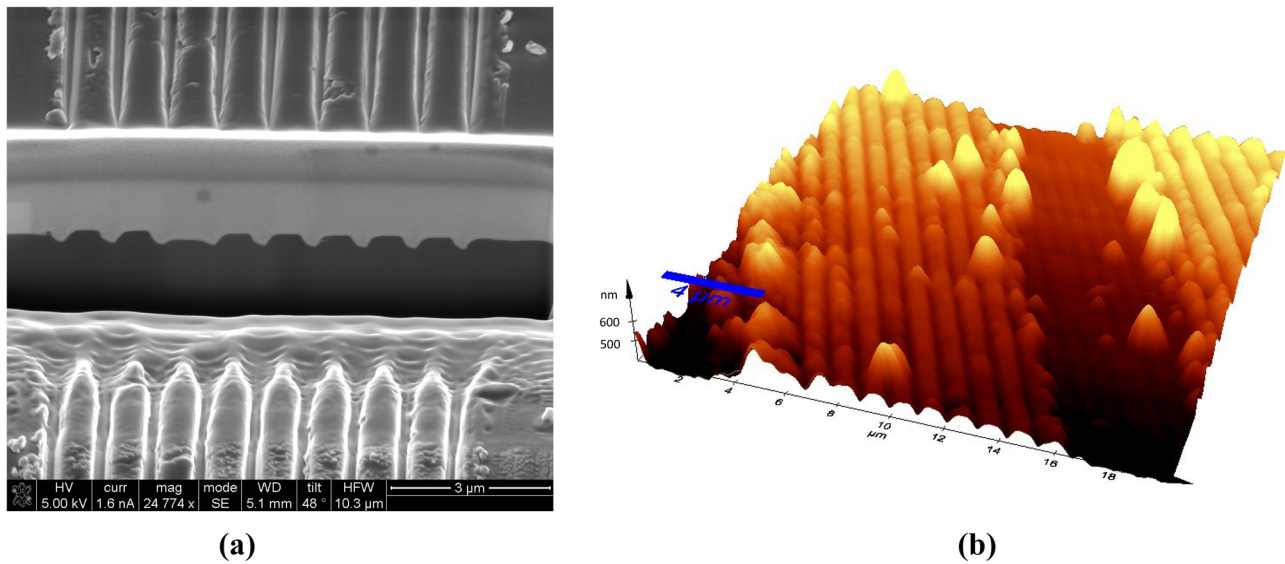


Fig. 5 (a) Nanostructured surface carved with FIB showing the profile of the nanochannels, (b) AFM measurement of the grooves

and t_u equals to feed per revolution. The specific cutting energy at 70 nm/rev can be calculated around 22 GPa which is a measure material's resistance to cutting. The thrust force measurements can be used to calculate the pressure at the cutting zone, which is shown in Fig. 9b. At 70 nm/rev feed, which is the same as previous tests, pressure for non-structured tools was calculated to be around 25–30 GPa which is lower than the viable pressure range

reported in [8]. With increasing feed, the pressure drops to around 13 GPa, which is just above the phase transformation pressure of silicon. Increasing tensile stresses on the surface due to larger feed starts micro-fractures on the surface.

The different trends in pressure with increasing cutting speed at 70 and 250 nm/rev feed may be related to the combined effect of thermal softening of the material due

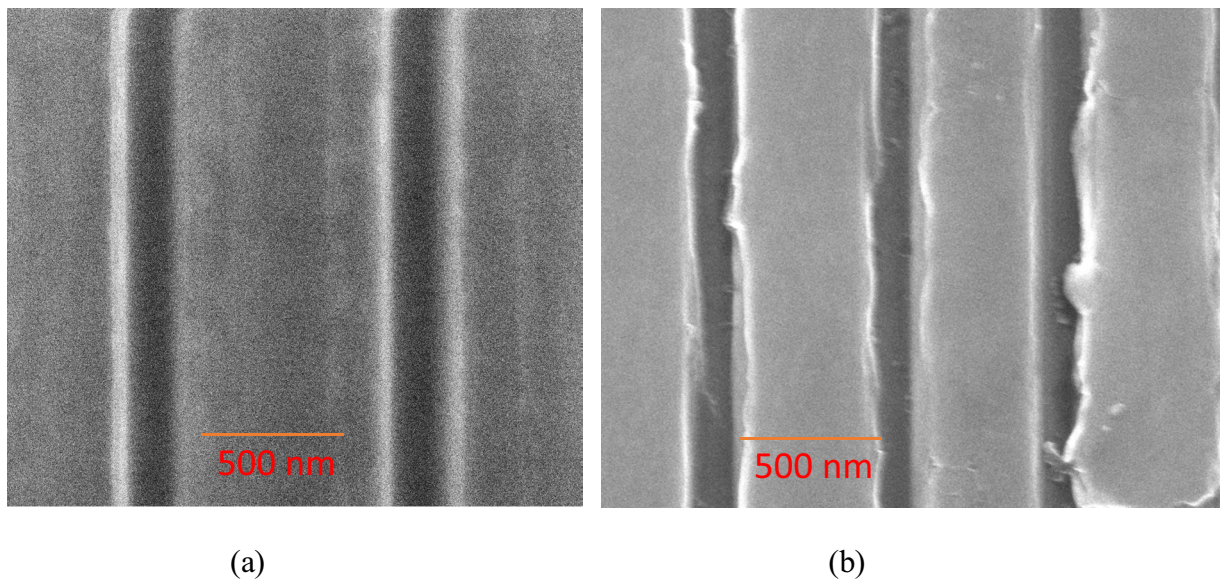


Fig. 6 (a) First group of nanogrooves exhibiting material pile-up, (b) second group of nanogrooves with large depth exhibiting fractured regions up ($V=25$ m/min, $f=70$ nm/rev), (c) Raman spectra of the different nanostructured surfaces compared with reference surface

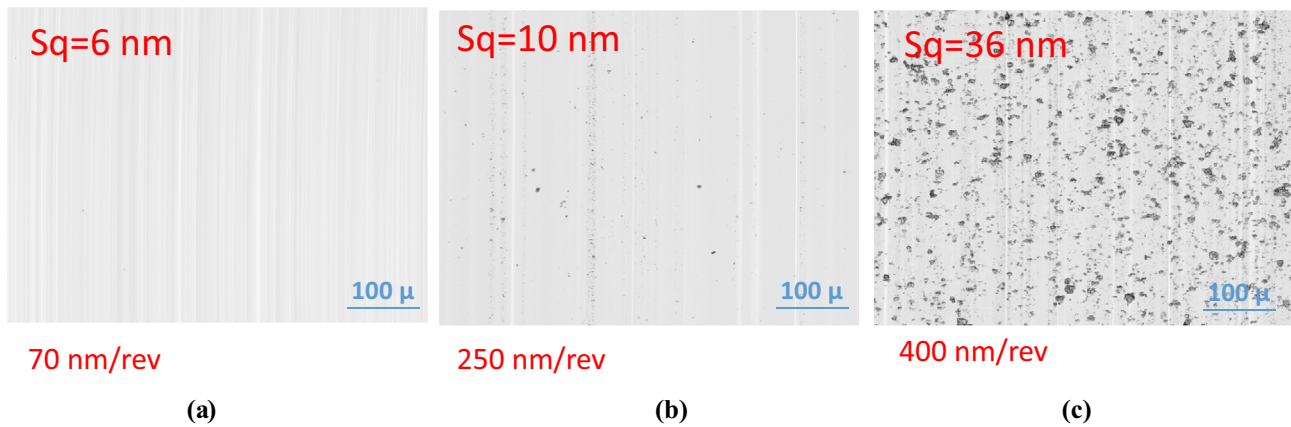


Fig. 7 Surface topology of the micro-grooves having 20 μm depth, (a) feed 70 nm/rev, (b) 250 nm/rev, (c) 400 nm/rev

to increasing temperature at the cutting zone and material strengthening due to increasing strain rate [12]. Pala et al. [15] developed a flash temperature model for diamond wire cutting of silicon. They showed that at nanometric cutting depths, flash temperatures would reach to up to 2500 K. The measured cutting forces correspond to 1.6 mN/ μm . At low feeds, the thrust (F_t)(or passive) force measurements are larger than the cutting forces, which indicates high apparent coefficient of friction ($\mu = \tan(\beta) = F_t/F_c$) at the tool-work material interface. The coefficient of friction with nanostructured tools would be higher compared

to non-structured tools due to increase area of contact during cutting.

The influence of machined nanostructures on the reflectivity of silicon is shown in Fig. 10. The measurements were conducted between 1000 and 2500 nm wavelength using Cary 5000 UV–Vis–NIR spectrophotometer. Compared to non-structured silicon surface, the positive influence of nanostructuring can be seen in the measurements. Additional research is required to evaluate the effect of dimensions of nanostructures on the reflectivity of the surface.

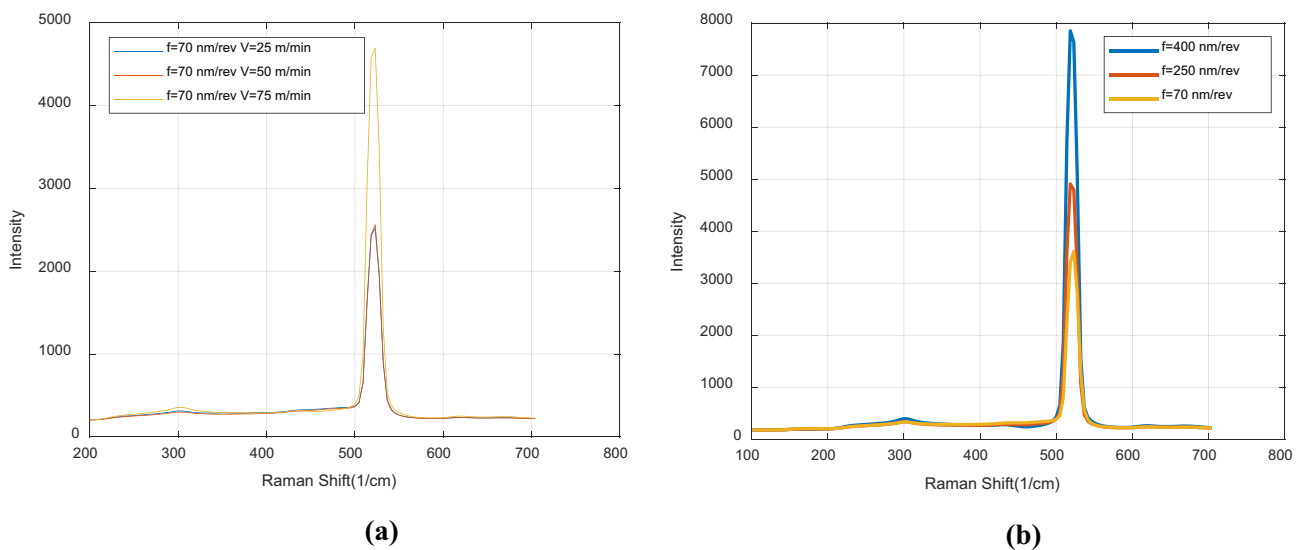
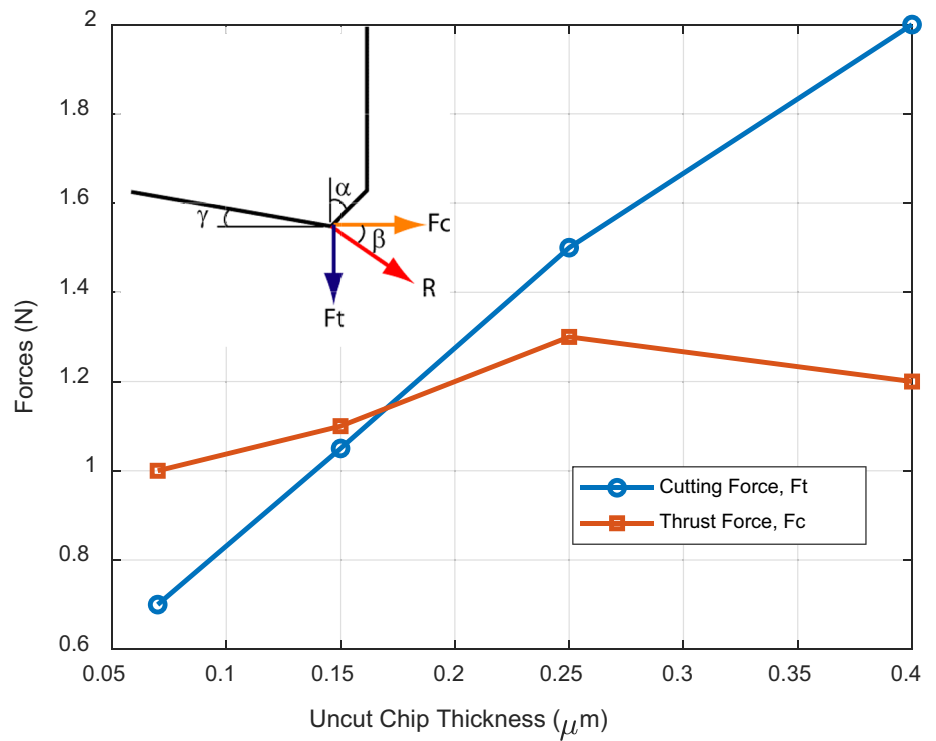
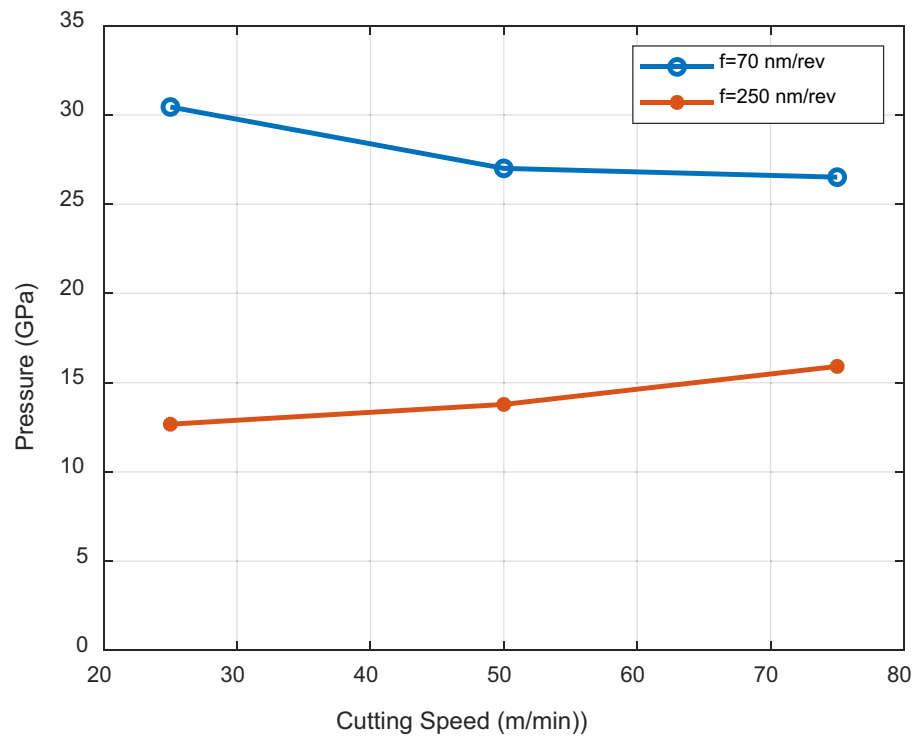


Fig. 8 Raman spectra of the machined surface with non-structured tool: (a) as a function of cutting speed, (b) as a function of feed at 25 m/min cutting speed

Fig. 9 (a) Measured cutting and thrust forces as a function of feed. The directions of the forces acting on the tool are also shown in the graph, (b) variation of hydrostatic pressure at the cutting zone as a function of feed and cutting speed

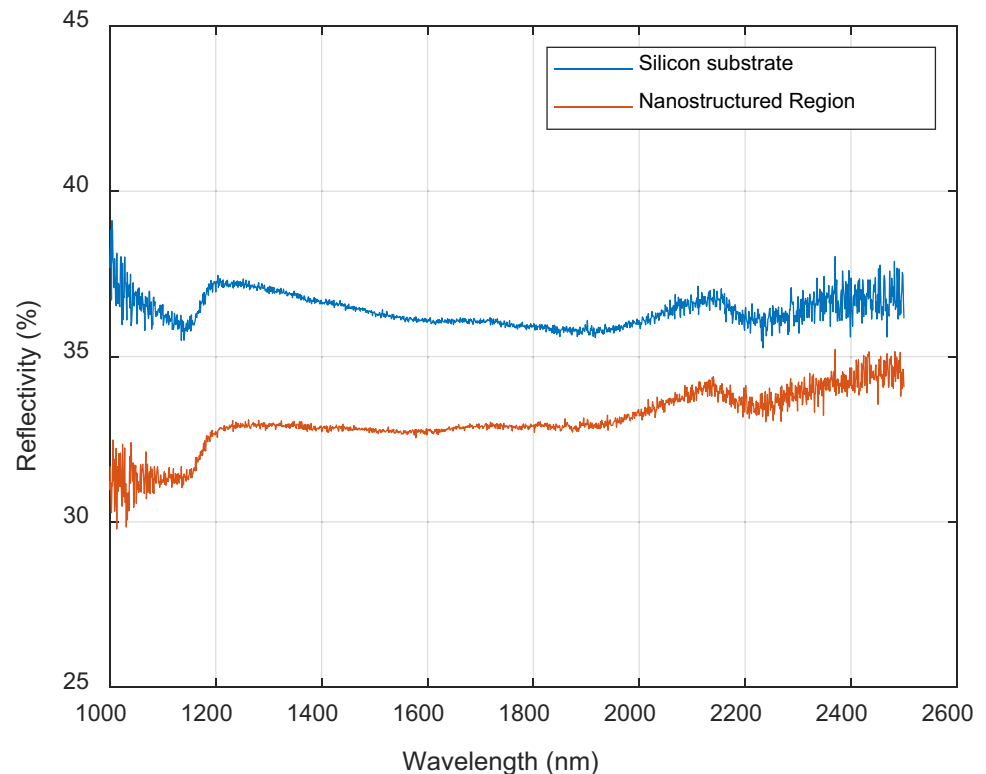


(a)



(b)

Fig. 10 Influence of nanostructuring on the reflectivity of the silicon surface



4 Conclusions

This study investigated the influence of nanoscale machining on the surface integrity of single crystal silicon. The findings of this study are given below:

- With increasing nanogroove depth, at 300 nm depth, hexagonal Si phase transformation was observed. This phase transformation has been linked to shear-induced plastic deformations created under high pressures and high coefficient of friction because of multi-tip structure of the tool.
- High cutting speed machining tests with non-structured diamond tools were conducted to better understand the phase transformations observed in machining with nanostructured tools. Cutting speed was increased to promote higher temperatures yet the analysis of the machined surface did not present any hexagonal-Si phase transformation. The pressures may not be high enough to initiate the Si-IV phase transformation. The annealing effect of temperature rise must be considered well.
- The design of the multi-tip tool considered in this study can machine single crystal silicon in ductile mode to create nano features as large as 90 nm height and 200 nm width. With increasing depth, nanogrooves as deep as

300 nm were obtained accompanied with some fractured regions.

- If successfully applied, significantly high material removal rates can be obtained with multi-tip, nanoscale diamond tools under ductile conditions. However, advanced tool tip location sensing techniques are required to control the location and dimensions of the nanogrooves. Tool wear of expensive diamond tools is another important issue to consider for practical applications.

Acknowledgements The author would like to thank Dr. Kıvanç Güngör and Mr. Mustafa Güler for their assistance during FIB machining process.

Author contribution Y. Karpaz: conceptualization, planning and conducting experiments, data processing and analysis, surface measurement, preparation of the original manuscript.

Funding This work was supported by the Turkish Scientific and Technological Research Council of Turkey (TUBITAK) through projects 115M699 and 218M431.

Declarations

Consent for publication The author consent to publishing the present study.

Competing interests The author declares no competing interests.

References

1. Fang FZ, Zhang XD, Gao W, Guo YB, Byrne G, Hansen HN (2017) Nanomanufacturing—perspective and applications. *CIRP Ann Manuf Technol* 66:683–705
2. Tong Z, Liang Y, Jiang X, Luo X (2014) An atomistic investigation on the mechanism of machining nanostructures when using single tip and multi-tip diamond tools. *Appl Surf Sci* 290:458–465
3. Tong Z, Luo X, Sun J, Liang Y, Jiang X (2015) Investigation of a scale-up manufacturing approach for nanostructures by using a nanoscale multi-tip diamond tool. *Int J Adv Manuf Technol* 80:699–710
4. Goel S, Luo X, Agrawal A, Reuben RL (2015) Diamond machining of silicon: a review of advances in molecular dynamics simulation. *Int J Mach Tools Manuf* 88:131–164
5. Tong Z, Luo X (2015) Investigation of focused ion beam induced damage in single crystal diamond tools. *Appl Surf Sci* 347:727–735
6. Chavoshi SZ, Goel S, Luo X (2016) Influence of temperature on the anisotropic cutting behaviour of single crystal silicon: a molecular dynamics simulation investigation. *J Manuf Process* 23:201–210
7. Dai H, Chen G, Zhou C, Fang Q, Fei X (2017) A numerical study of ultraprecision machining of monocrystalline silicon with laser nano-structured diamond tools by atomistic simulation. *Appl Surf Sci* 393:405–416
8. Paul R, Hu SX, Karasiev VV (2019) Crystalline phase transitions and vibrational spectra of silicon up to multi tera pascal pressures. *Phys Rev B* 100:144101
9. Fan L, Yang D, Li D (2021) A review on metastable silicon allotropes. *Materials* 14:3964. <https://doi.org/10.3390/ma14143964>
10. Pandolfi S, Renero-Lecuna C, Le Godec Y, Baptiste B, Menguy N, Lazzeri M, Gervais C, Spektor K, Crichton WA, Kurakevych OO (2018) Nature of hexagonal silicon forming via high-pressure synthesis: nanostructured hexagonal 4H polytype. *Nano Lett* 18(9):5989–5995. <https://doi.org/10.1021/acs.nanolett.8b02816>
11. Domnich V, Gogotsi Y (2002) Phase transformations in silicon under contact loading. *Rev Adv Mater Sci* 3:1–36
12. Wang B, Melkote SN, Wang P, Saraogi S (2020) Effect of speed on material removal behavior in scribing of monocrystalline silicon. *Precis Eng*. <https://doi.org/10.1016/j.precisioneng.2020.07.011>
13. Dahmen U, Hetherington CJ, Pirouz P, Westmacott KH (1989) The formation of hexagonal silicon at twin intersections. *Scr Metall* 23:269–272
14. Vincent L, Djomani D, Fakfakh M, Renard C, Belier B, Bouchier D, Patriarche G (2018) Shear-driven phase transformation in silicon nanowires. *Nanotechnology* 29:125601
15. Pala U, Süßmaier S, Wegener K (2021) Grain flash temperatures in diamond wire sawing of silicon. *Int J Adv Manuf Technol* 117:2227–2236

Publisher's Note Springer Nature remains neutral with regard to jurisdictional claims in published maps and institutional affiliations.